An Experimental and Computational Study of the Aerodynamics of a Square Cross-Section Body at Supersonic Speeds

Trevor J. Birch, Simon A. Prince and Graham M. Simpson
Aerodynamics Department, DERA, Bedford MK41 6AE, United Kingdom

Abstract

An experimental and computational study has been carried out to investigate the aerodynamic characteristics of a square cross-section body at supersonic speeds. The results show that a square cross-section body generates higher normal force and offers improved lift-to-drag ratios when compared with conventional circular cross-section bodies for certain preferred orientations. However it was found that square cross-section bodies can also generate significant lateral forces and moments, and very complicated leeside vortical flowfields which complicate the missile control system. A Parabolized Navier-Stokes solver was successfully employed to predict the forces and moments, and provided added valuable insight into the complex vortical flows which develop on the leeside of bodies at incidence.

Introduction

The vast majority of guided weapons favour a symmetric cruciform layout and utilise a circular cross-section fuselage with aerodynamic surfaces added to provide stability and control. In recent years there has been an increasing interest in weapons having non-axisymmetric airframes driven by the need for improved kinematic performance, low observability, and better weapon/aircraft integration, particularly for internal carriage.

Square cross-section bodies have been found to offer some aerodynamic advantages over equivalent axisymmetric bodies, and when oriented with the incidence plane passing through opposite corners, they can provide higher values of normal force and lift-drag ratio[1]. However, the aerodynamic characteristics are roll dependent, and at asymmetric roll orientations square cross-section bodies can produce significant, and unwanted, side forces and yawing moments.

In this paper experimental force and moment data for a square cross-section body are presented and compared with an equivalent axisymmetric body over the Mach number range 2.5 to 4.5. This extends the results of Brebner, Osborne and Brown[1], who obtained data for the same configuration over the Mach number range 0.6 to 2.0.

The experimental data have been used to evaluate the predictive performance of a Parabolized Navier-Stokes solver for square cross-section bodies. Having proved the capability of the PNS solver for this geometry it was then used to provide insight into the complex flowfields surrounding a square cross-section body and to investigate the effect of varying the body fineness ratio.

Paper presented at the RTO AVT Symposium on "Advanced Flow Management: Part A – Vortex Flows and High Angle of Attack for Military Vehicles", held in Loen, Norway, 7-11 May 2001, and published in RTO-MP-069(I).

Report Documentation Page

Form Approved
OMB No. 0704-0188

1. REPORT DATE	2. REPORT TYPE	3. DATES COVERED
00 MAR 2003	**N/A**	**-**

4. TITLE AND SUBTITLE	5a. CONTRACT NUMBER
An Experimental and Computational Study of the Aerodynamics of a Square Cross-Section Body at Supersonic Speeds	5b. GRANT NUMBER
	5c. PROGRAM ELEMENT NUMBER
6. AUTHOR(S)	5d. PROJECT NUMBER
	5e. TASK NUMBER
	5f. WORK UNIT NUMBER
7. PERFORMING ORGANIZATION NAME(S) AND ADDRESS(ES) **NATO Research and Technology OrganisationBP 25, 7 Rue Ancelle, F-92201 Neuilly-Sue-Seine Cedex, France**	8. PERFORMING ORGANIZATION REPORT NUMBER
9. SPONSORING/MONITORING AGENCY NAME(S) AND ADDRESS(ES)	10. SPONSOR/MONITOR'S ACRONYM(S)
	11. SPONSOR/MONITOR'S REPORT NUMBER(S)

12. DISTRIBUTION/AVAILABILITY STATEMENT
Approved for public release, distribution unlimited

13. SUPPLEMENTARY NOTES
Also see: ADM001490, Presented at RTO Applied Vehicle Technology Panel (AVT) Symposium held inLeon, Norway on 7-11 May 2001, The original document contains color images.

14. ABSTRACT

15. SUBJECT TERMS

16. SECURITY CLASSIFICATION OF:			17. LIMITATION OF ABSTRACT	18. NUMBER OF PAGES	19a. NAME OF RESPONSIBLE PERSON
a. REPORT	b. ABSTRACT	c. THIS PAGE			
unclassified	**unclassified**	**unclassified**	**UU**	**14**	

Geometry details

The bodies studied are shown in figure 1. The axisymmetric body consisted of a 3 calibre nose having a cubic profile, followed by a 10 calibre cylindrical section of diameter 3.7" (93.98mm). The nose profile is similar to a tangent-ogive and is given by the following equation:

$$r/D = -0.002615(x/D)3 -0.039867(x/D)2 +0.30984(x/D),$$

where r is the nose radius at a distance x from the apex. The square cross-section body had a pyramidal nose of length 3D and a total length of 13D. The maximum dimension of a side of the body cross-section was 1D.

Experimental details

Wind tunnel tests were conducted in the High Supersonic Speed Tunnel (HSST) at DERA Bedford. This is a closed-circuit, continuous-flow, variable density supersonic facility with a working section of 3ft by 4ft. Forces and moments were measured over the Mach number range 2.5 to 4.5 using a six-component strain gauge balance. The test Reynolds number was 1.2×10^6 based on D.

Computational details

The iterative PNS solver, IMPNS, was used for all computations. This code has evolved over a number of years and has been developed primarily for predicting the aerodynamic characteristics of missiles and projectiles travelling at supersonic speeds[2-5].

In each crossflow plane, the inviscid fluxes are computed using the approximate Riemann solver of Osher and Solomon. Spatial accuracy is enhanced to nominally third-order by a MUSCL primitive variable extrapolation scheme. In the streamwise direction second-order accuracy is achieved outside of the boundary layer by use of a (non slope-limited) primitive variable extrapolation. The PNS equations are solved on each crossflow plane using pseudo-time relaxation. In order to accelerate convergence various implicit schemes can be used with or without multigrid. In the present study the effects of turbulence were modelled using the Baldwin-Lomax model with the modifications for vortical flows of Degani and Schiff.

All computations were completed on structured body conforming grids. For the symmetric roll orientations (λ=0° and 45°) only one half of each configuration was modelled to reduce code execution times. Each of the half model grids consisted of 89 points in the streamwise, radial and circumferential directions. For the asymmetric roll cases the half grids were mirrored about the pitch plane.

Results

The overall force and moment coefficients have been resolved in a body axis system which does not roll with the body. The axis system is shown in figure 2. The reference length used was D. The reference area was $\pi D^2/4$ for the circular cross-section body and D^2 for the square cross-section body. The pitching and yawing moment reference centre was on the body axis at x=0.0.

Longitudinal Characteristics

The measured and predicted longitudinal aerodynamic characteristics for the square and circular cross-section bodies are compared in figures 3 and 4 for Mach numbers of 2.5 and 4.5 respectively. At all non-zero incidence angles, and both Mach numbers, the normal force

coefficient is greatest for the square cross-section body when oriented at λ=45°. When oriented at λ=0° (flat side windward) the normal force for the square cross-section body is a minimum, but is still slightly higher than for the circular cross-section body. At σ=14^o and M=2.5 the normal force for the square cross-section body at λ=45° is 53% greater than for the circular cross-section body, but reduces to about 28% at M=4.5. The centre of pressure is further aft for the square cross-section body and is less sensitive to variations in incidence.

The axial force acting on the square cross-section body is greater than that on the circular body, and is almost constant with roll at the lower Mach number. The lift-to-drag ratio for the square cross-section at λ=0° is very similar to that for the equivalent circular body. However, when oriented at λ=45° the lift-to-drag ratio is considerably improved. Table 1 shows the maximum lift-to-drag ratio and the incidence at which it occurs for both bodies at M=2.5 and 4.5.

The predicted normal force and longitudinal centre of pressure are generally in good agreement with experiment for both Mach numbers over the complete incidence range. The predicted axial forces are consistently lower than the measured values, although the trends with incidence are correct. This is probably due to the simple turbulence model, which has previously been found to underpredict the skin friction contribution to axial force[6].

Figure 5 compares the predicted leeside flowfield in a crossflow plane at x/D=11.5 for σ=14^o for the circular and square cross-section bodies. Measured data for the circular cross-section body are included in this figure to confirm the reliability of the CFD predictions. It can be seen that the predicted flowfield above the circular cross-section body is in good agreement with experiment. The predictions for the square cross-section body should also be reliable. The flow separates at the sharp corners on the square cross-section body at both Mach numbers. At M=2.5 and λ=0° this results in a large separated region along the entire side of the body, and a leeside vortex. The flowfield at λ=45° remains attached until the sharp corner is encountered, at which point it separates and rolls-up to form a strong leeside vortex. This remains close to the body surface and a secondary vortex is formed. The flowfields at M=4.5 are broadly similar, but the body vortices are more diffuse, and as the crossflow is supersonic, the flowfields also include embedded crossflow shock waves.

Lateral Characteristics

It has already been shown that the normal force acting on the square cross-section body varies considerably with roll angle. This is also the case for side force and yawing moment, and even at small angles of incidence, asymmetric roll angles can result in significant lateral forces and moments. Figure 6 shows the variation of side force and yawing moment coefficient with roll angle for the square cross-section body, at M=2.5 and 4.5, and σ=14°. The maximum side force and yawing moment occur at approximately λ=22.5°. The side force coefficients predicted using the PNS code are in good agreement with the measured data. The predicted yawing moments are not as good. Although, as for the side force there is some scatter in the measured data.

The computed flowfields, at a plane at x/D=11.5, for the square cross-section body at M=2.5 and σ=14° are compared in figure 7 for various roll orientations. In all cases the flowfields are dominated by leeside vortices. For asymmetric roll orientations these vortices interact and form complex flowfields. The associated leeside surface pressures make a significant contribution to the lateral forces and moments.

In figure 8 computed values of accumulative normal, side and axial force coefficient are plotted along the axial length of the square cross-section body, for M=2.5, σ=14° and a non-

symmetric roll angle of 22.5°. It can be seen that the magnitude of the side force can be as much as 24% of the normal force for the 13D body, even at this modest incidence. Calculations were completed on longer bodies (beyond x/D=13) to provide an indication of how the aerodynamic characteristics vary with fineness ratio. The majority of the side force is generated beyond x/D=6. The predicted local force distributions are presented for the same maximum side force condition at $\lambda=22.5^{o}$, in figure 9. The maximum side force contribution occurs near x/D=10, and corresponds with a plateau in the local normal force distribution. This suggests that both forces are being influenced by a vortex that is being shed from the body in this region.

The computed flowfields at several longitudinal positions along the square cross-section body are presented in figure 10 for M=2.5, $\sigma=14°$ and $\lambda=22.5°$. The flowfield surrounding the body is extremely complex, and features multiple vortices which are influencing the body surface pressures, and consequently, the overall forces and moments. Between x/D=9 and x/D=13 the main leeside vortex grows to its maximum size, which corresponds with the peak in local side force, and is then shed. As the vortex moves away from the body its effect on the local surface pressure reduces and a new vortex forms.

The complex vortex flowfield surrounding a square cross-section body could lead to problems when aerodynamic surfaces are added to provide stability and control. The vortex dominated flows are likely to result in unwanted vortex-fin interference and complex pitch-yaw cross coupling.

Conclusions

A square cross-section body can generate significantly greater normal force and offer improved lift-to-drag ratios when compared with a conventional circular cross-section body for certain preferred orientations.

Square cross-section bodies, even at modest incidence angles, can generate significant lateral forces and moments for non-symmetric roll orientation. These characteristics will increase the necessary complexity of any control system.

The flowfields surrounding a square cross-section body are generally more complex than for an equivalent axisymmetric body, making the integration of aerodynamic surfaces, or air intakes very challenging.

A PNS solver has been successfully used to predict the forces and moment on a square cross-section body at supersonic speeds. The results of these computations have provided valuable insight into the physics of the complex flows around square cross-section bodies.

References

1. Brebner, G. G.; Osborne, W. K.; Brown, D. E. Force and Moment Wind Tunnel Measurements at Mach Numbers From 0.6 to 2.0 on a Body of Square Cross-Section, Alone and in Combination with Cruciform Delta Wings of Aspect Ratio 0.52. RAE TR 81035, March 1981.

2. Birch, T. J., Qin, N. and Jin, X., Computation of Supersonic Viscous Flows Around a Slender Body at Incidence, AIAA Paper 94–1938, 1994.

3. Shaw, S. T., and Qin, N., A Matrix-free Preconditioned Krylov Subspace Method for the PNS Equations, AIAA Paper 98–0111, 1998.

4. Qin, N., Ludlow, D. K., Zhong, B., Shaw, S., and Birch, T. J., Multigrid Acceleration of a Preconditioned GMRES Implicit PNS Solver, AIAA Paper 99-0779, 1999.

5. Birch, T.J., Ludlow, D, K, and Qin N., Towards an Efficient, Robust and Accurate Solver for Supersonic Viscous Flows, ICAS 2000 Paper 242, 2000.

6. Birch, T.J., Wrisdale, I. E., and Prince, S.A., CFD Predictions of Missile Flowfields, AIAA Paper 2000-4211, 2000.

Body	**Mach Number**	**L/D_{max}**	**σ**
Circular cross-section	2.5	2.78	12.5
	4.5	2.98	10.0
Square (λ=0°)	2.5	2.79	12.0
	4.5	2.94	9.5
Square (λ=45°)	2.5	3.23	10.0
	4.5	3.35	9.0

Table 1. Conditions at maximum L/D

Figures

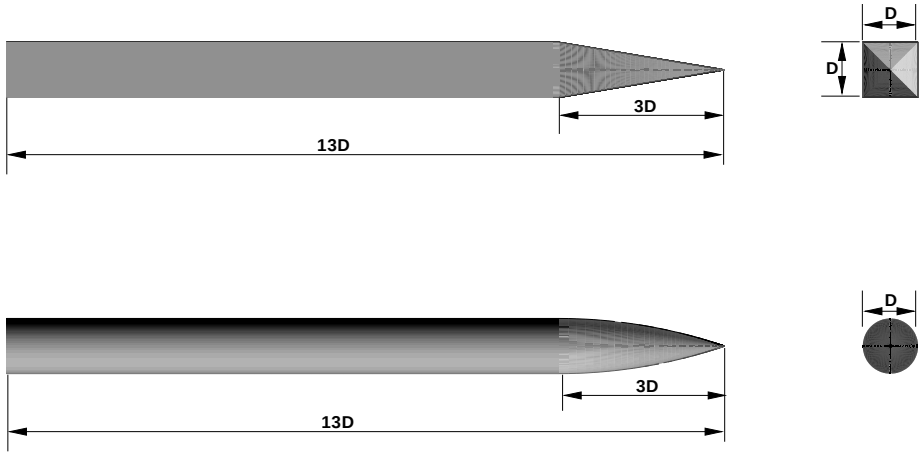

Figure 1: Square cross section and tangent-ogive cylinder body geometry

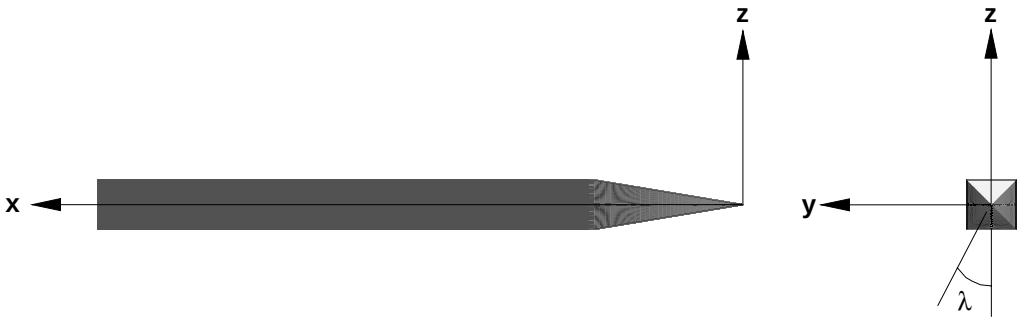

Figure 2: Body axis system (non rolling)

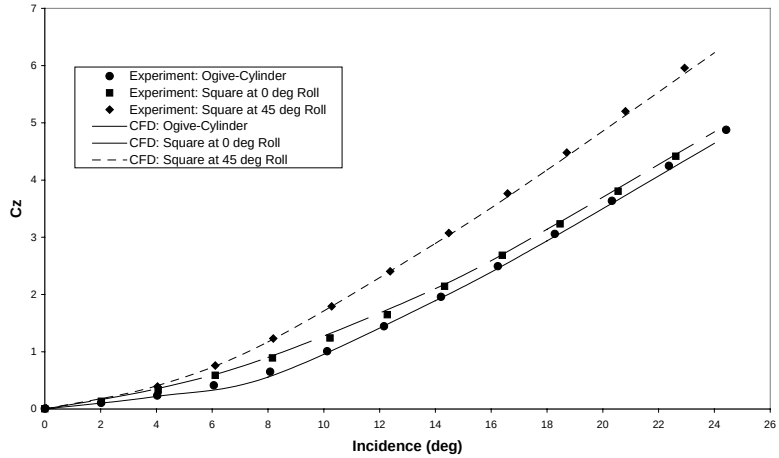

a) Normal force coefficient

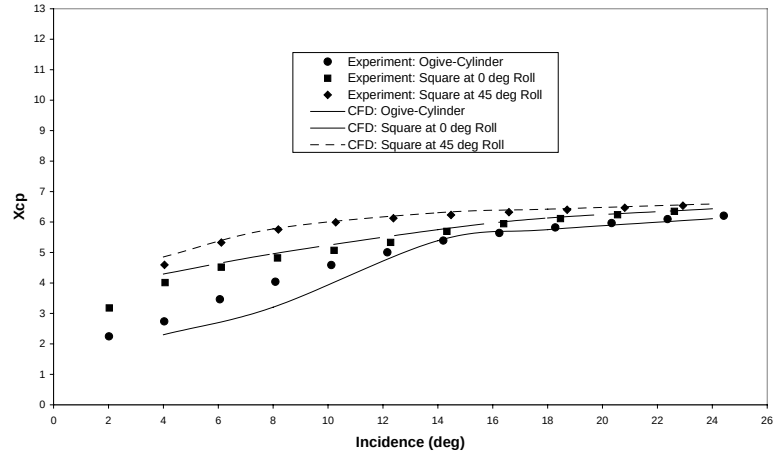

b) Centre of pressure position

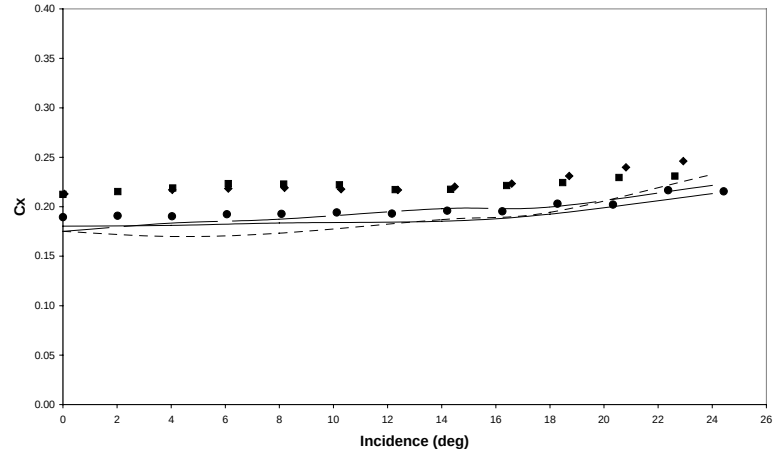

c) Axial force coefficient

Figure 3: Comparison of experimental and computationally predicted aerodynamics for square (0°and 45° roll) and circular cross-sectioned bodies at Mach 2.5.

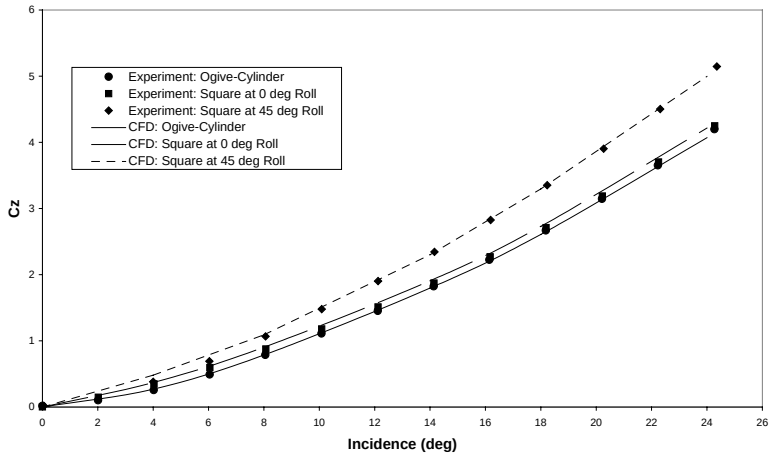

a) Normal force coefficient

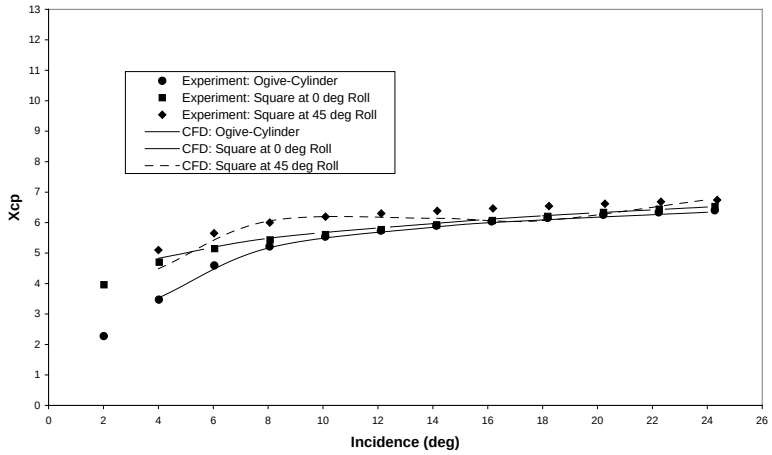

b) Centre of pressure position

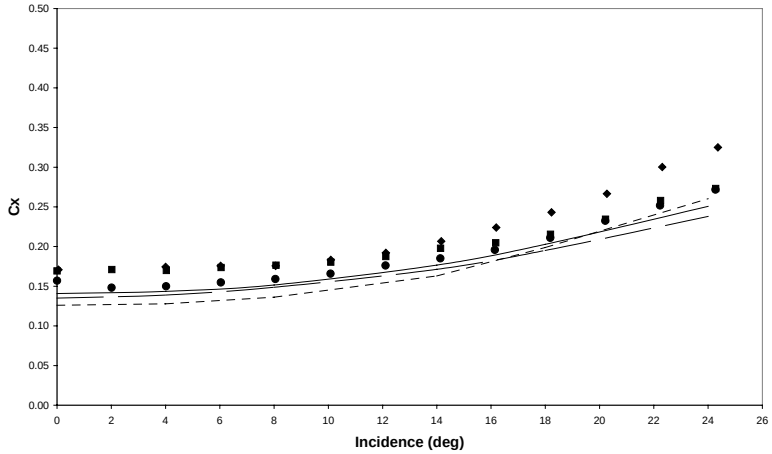

c) Axial force coefficient

Figure 4: Comparison of experimental and computationally predicted aerodynamics for square (0°and 45° roll) and circular cross-sectioned bodies at Mach 4.5.

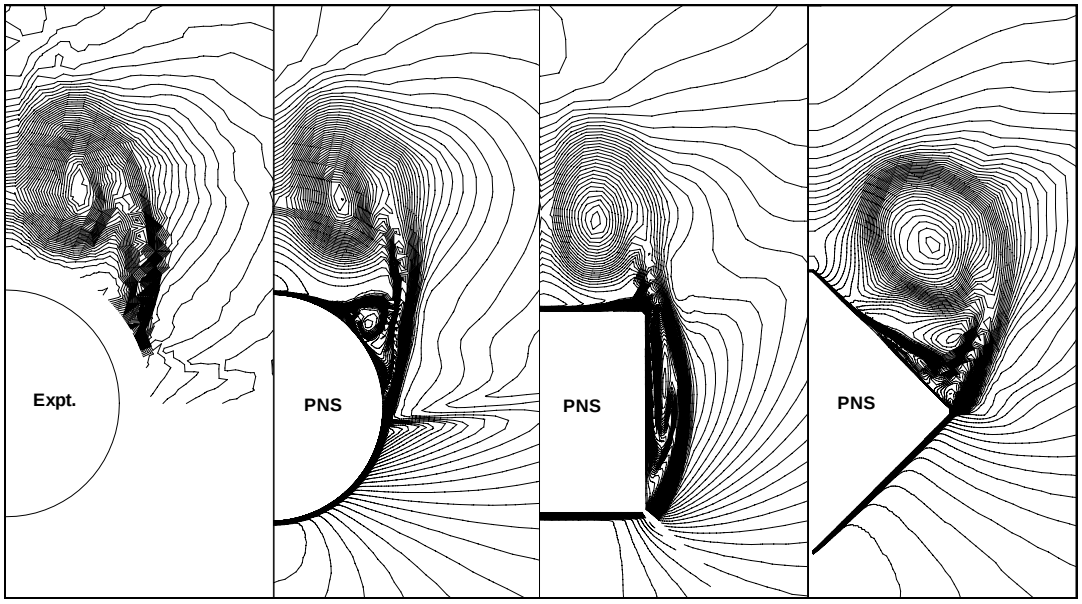

a) Mach 2.5

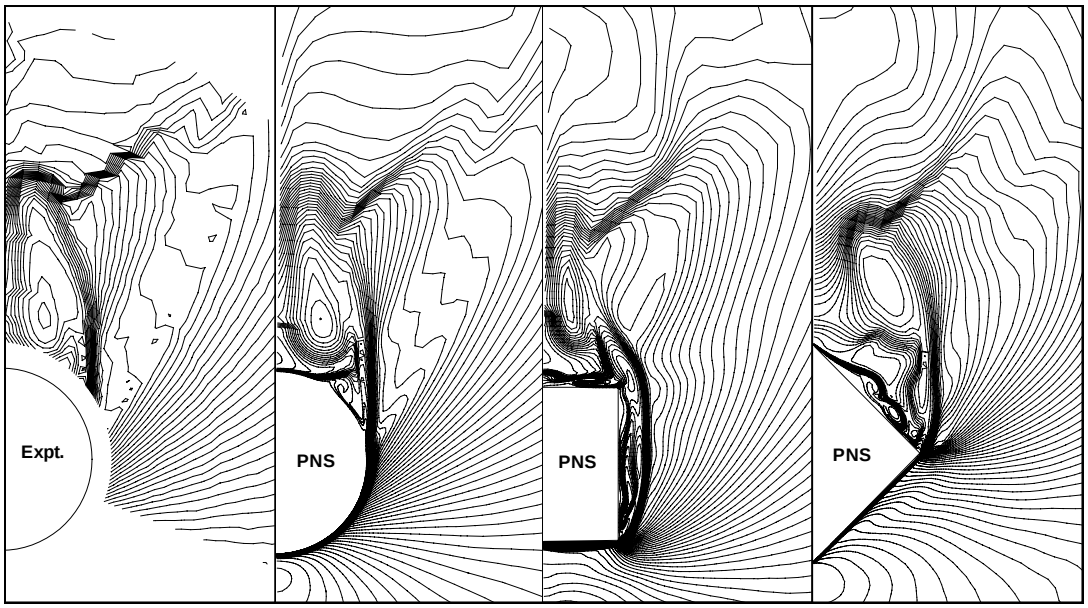

b) Mach 4.5

Figure 5: Pitot pressure contours in a cross flow plane at x/D=11.5, σ=14°.

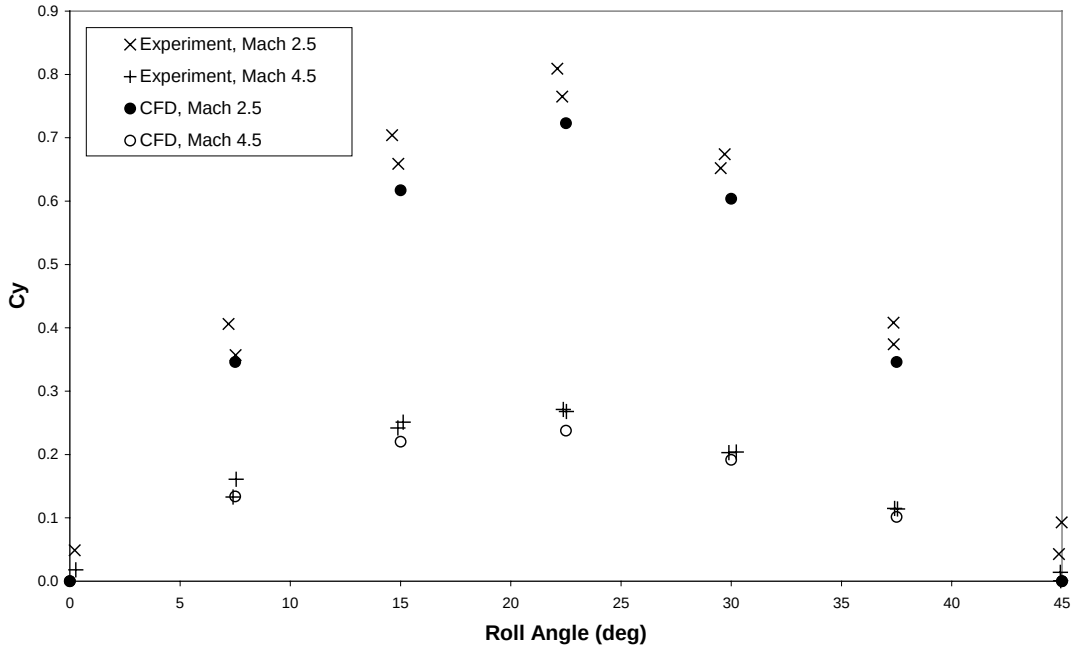

a) Side force

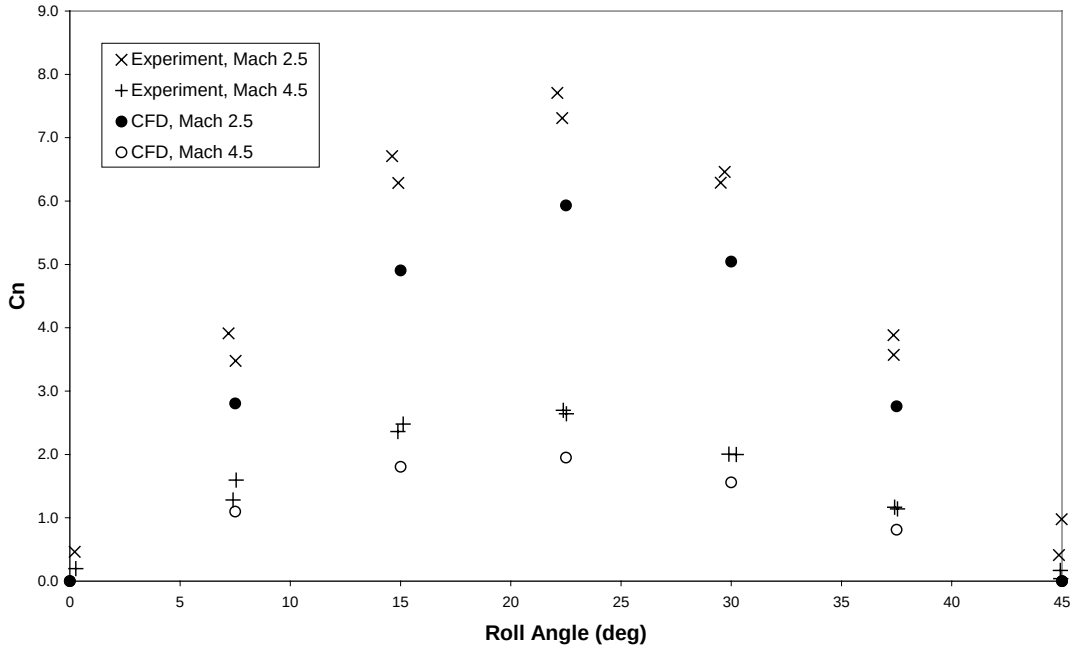

b) Yawing moment

Figure 6: Comparison of measured and predicted side force and yawing moment coefficients for the square cross-sectioned body at 14° incidence.

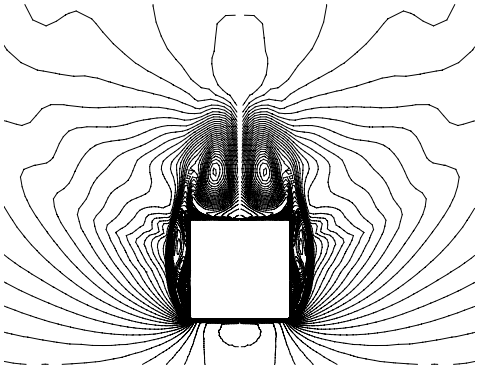

a) $\lambda = 0^o$ Roll

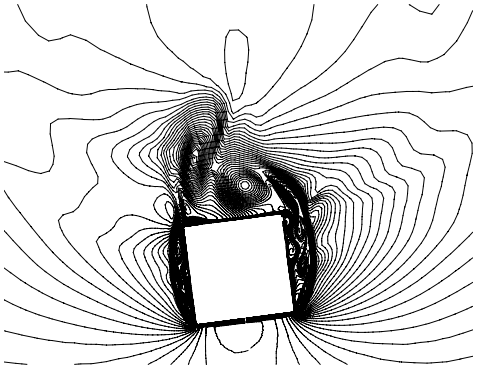

b) $\lambda = 7.5^o$ Roll

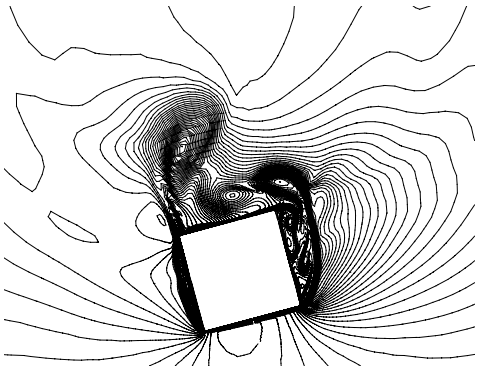

c) $\lambda = 15^o$ Roll

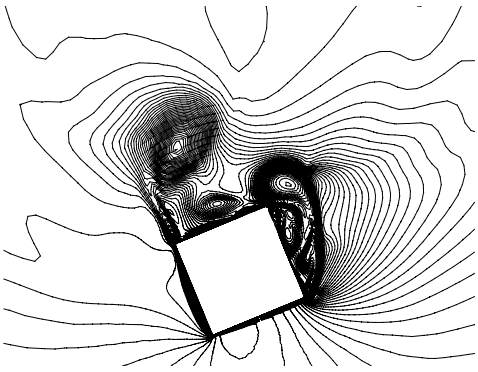

d) $\lambda = 22.5^o$ Roll

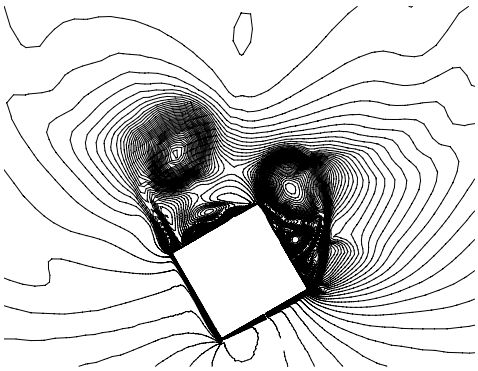

e) $\lambda = 30^o$ Roll

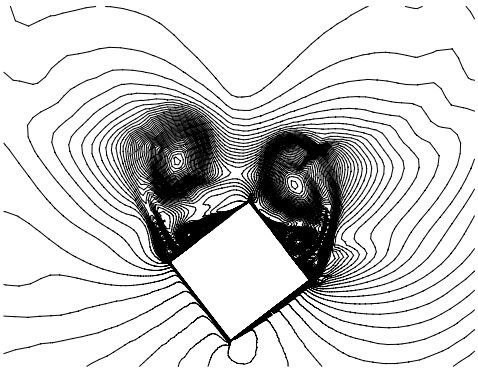

f) $\lambda = 37.5^o$ Roll

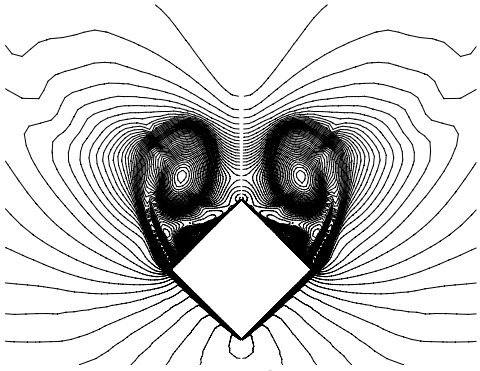

g) $\lambda = 45^o$ Roll

Figure 7: Computed pitot pressure contours for the square cross section body at 14° incidence, for the full roll sweep at M=2.5, x/D=11.5

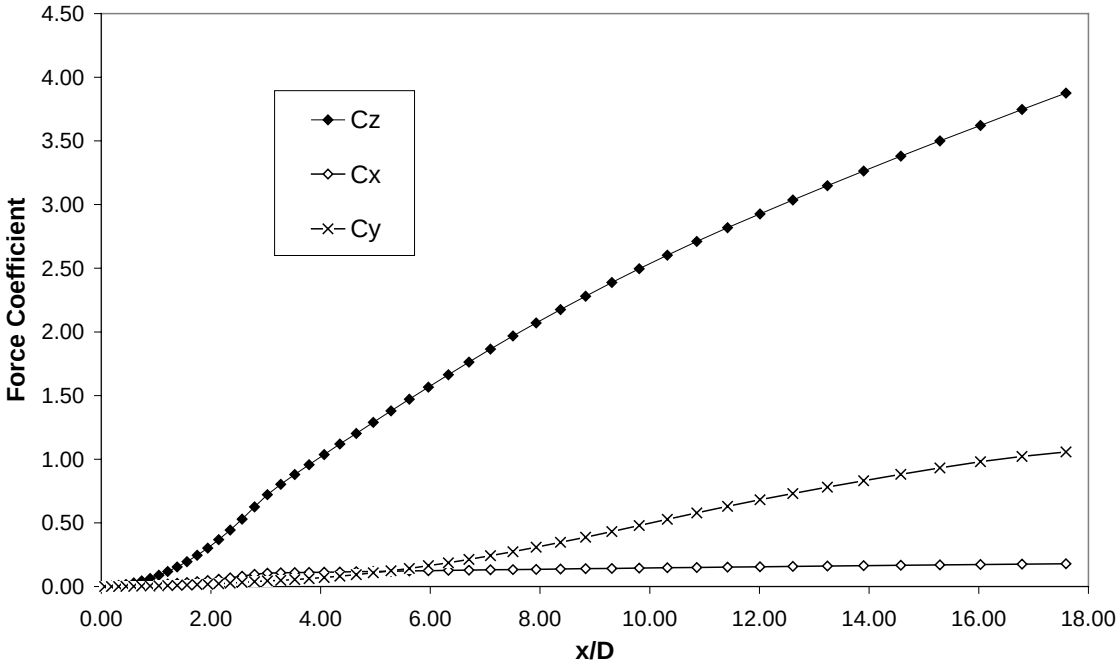

Figure 8: Accumulative force coefficients for the square cross section body at M=2.5, $\sigma=14^o$ and $\lambda=22.5^o$

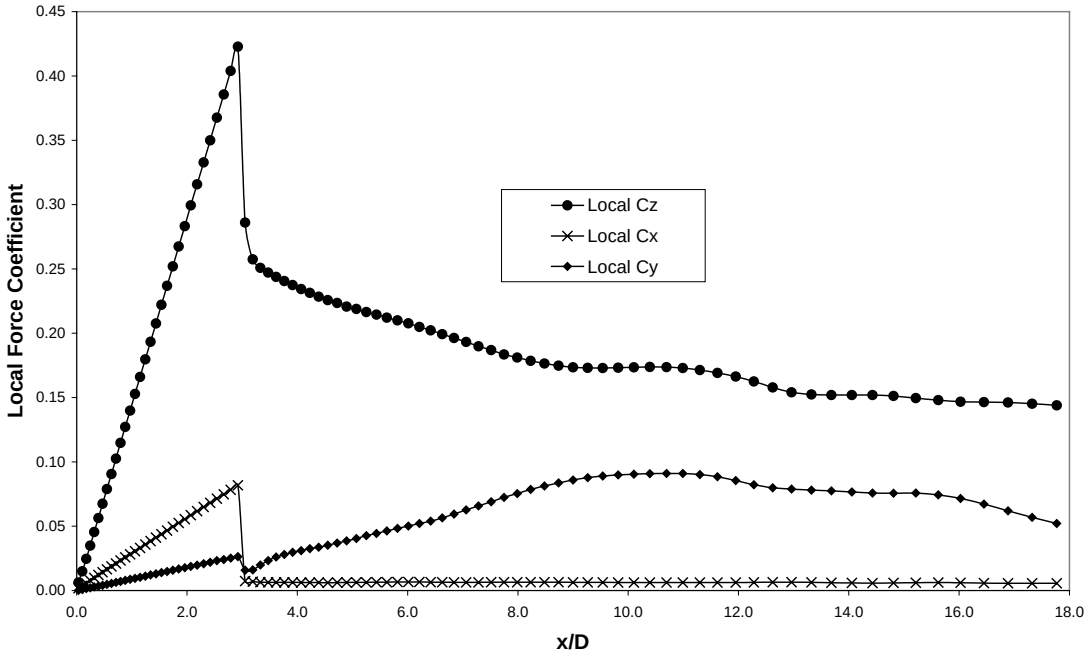

Figure 9: Local force coefficients for the square cross section body at M=2.5, $\sigma=14^o$ and $\lambda=22.5^o$

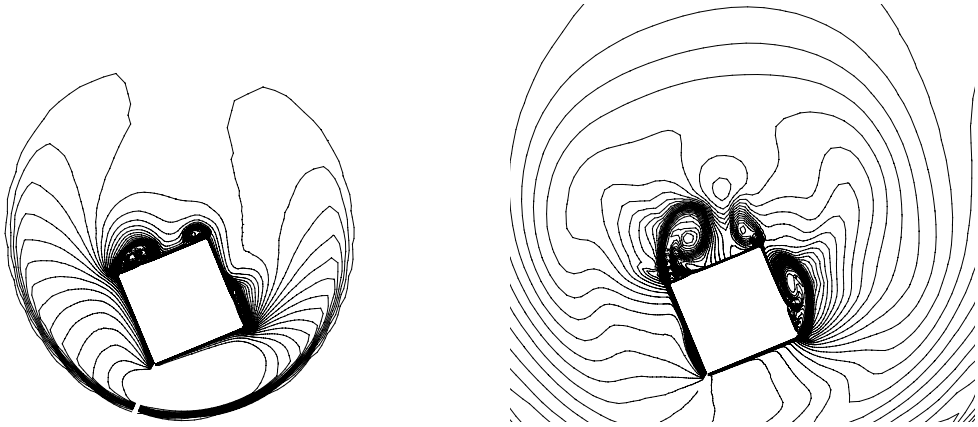

a) x/D=3

b) x/D=6

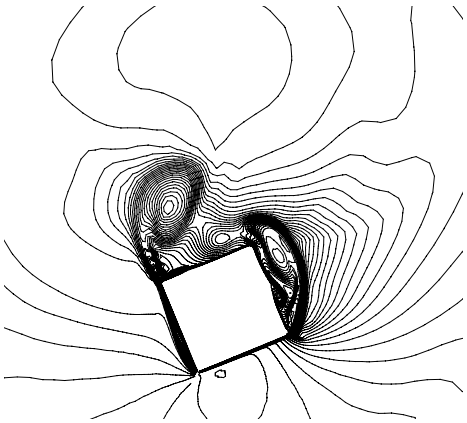

c) x/D=9

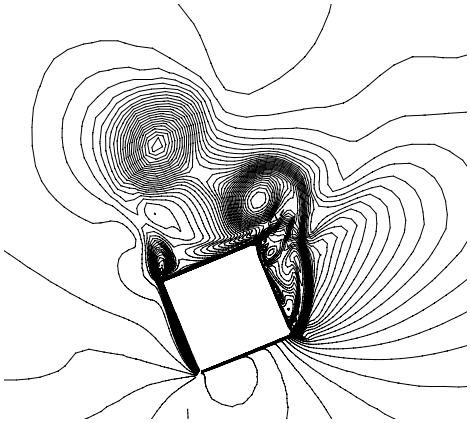

d) x/D=13

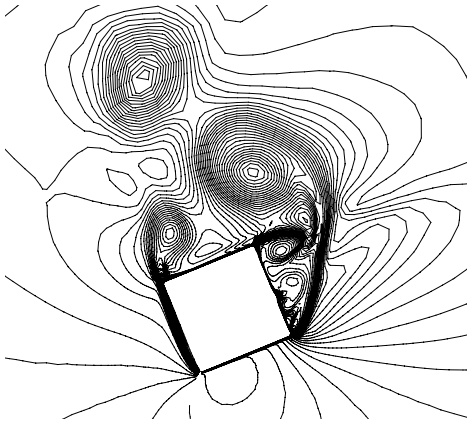

e) x/D=17.6

Figure 10: Computed pitot pressure contours for the square cross section body M=2.5, σ*=14°,* λ*=22.5°*

Paper: 3
Author: Mr. Birch

Question by Dr. Bredif: Can you comment about the lower limit for the Mach number range in your PNS code?

Answer: (No response recorded).

Question by Dr. Khalid: Was your computed flow field numerically steady, or did the presence of vortices and separation produce numerical oscillations in the convergence history?

Answer: Although the residual convergence on each plane was set for six orders, the first two or three planes would only converge to about five orders. However, no oscillatory mode of stalled convergence occurred, indicating no tendency toward an asymmetric vortex pattern.

Question by Dr. Luckring: Was there any treatment of numerical uncertainty in your work?

Answer: Grid sensitivity studies were done.